INTERNATIONAL JOURNAL OF ENERGY RESEARCH
Int. J. Energy Res. 2003; **27**:961–973 (DOI: 10.1002/er.928)

The onset of Darcy–Brinkman convection in a porous layer using a thermal nonequlibrium model—part I: stress-free boundaries

A. Postelnicu[a] and D.A.S. Rees[b,*]

[a] *Department of Thermo and Fluid Dynamics, Transylvania University of Brasov, Brasov 2200, Romania*
[b] *Department of Mechanical Engineering, University of Bath, Bath BA2 7AY, England, U.K.*

SUMMARY

The paper deals with the onset of convection in a porous layer heated from below, by considering the case when the fluid and solid phases are not in local thermal equilibrium and when form-drag and boundary effects are included in the analysis. Analytical progress is facilitated by taking stress-free boundaries conditions. Asymptotic solutions for both small and large values of the scaled inter-phase heat transfer coeffcient, H, are presented and comparisons with the numerical solutions are performed. Excellent agreement is obtained between the asymptotic and the numerical results. Copyright © 2003 John Wiley & Sons, Ltd.

KEY WORDS: porous medium; local thermal nonequilibrium; convection; linear stability

1. INTRODUCTION

The research presented here focuses on the porous medium version of the Bénard problem which has been studied extensively since the pioneering works of Horton and Rogers (1945) and Lapwood (1948) first appeared. Particular emphasis is given to the effects of including a two-field model for heat transport through the medium where the volume averaged temperature of the solid and fluid phases are generally different from one another. This effect is also known as local thermal non-equilibrium since, from a macroscopic point of view, thermal equilibrium does not occur even in steady-state convection, although it clearly must do at a microscopic level.

The earliest analysis of such non-equilibrium effects were presented by Schumann (1929) who considered a one-dimensional semi-infinite bed subject to a step-change in the inlet fluid temperature. Most of the more recent studies of thermal non-equilibrium effects have considered forced convective flows, and many of these have been reviewed in the chapters by Vafai and Amiri (1998) and Kuznetsov (1993). However, we are interested in the onset of free convection and the literature associated with this aspect is very limited. Combarnous (1972) performed

*Correspondence to: D.A.S. Rees, Department of Mechanical Engineering, University of Bath, Bath BA2 7AY England, U.K.
† E-mail: ensdasr@bath.ac.uk

Received 31 January 2002
Accepted 6 January 2003

finite difference calculations of the strongly non-linear flow and heat transfer in a unit square at only one Rayleigh number. More recently Banu and Rees (2002) considered the more general onset problem where criteria were sought to determine at what value of the Rayleigh convection would first occur.

In the present paper we extend the work of Banu and Rees (2002) by the inclusion of boundary effects as modelled by the Brinkman terms. Form-drag is also included, but it is quickly shown that these terms have no effect on stability criteria since the basic state whose stability is being analysed is one of no flow. We consider how non-LTE effects affect the onset criterion for the case of stress-free boundaries since, for these boundary conditions, it is possible to proceed entirely analytically as in Banu and Rees (2002). This assumption is relaxed in our companion paper (Rees and Postelnicu, 2002). We find that in both the LTE ($h \to \infty$) and non-LTE limits ($h \to 0$), the critical wave number tends towards π, but our analysis shows that at intermediate values of h, the critical wave number is always above π.

2. ANALYSIS

We consider a layer of porous medium with depth d which is heated from below and cooled from above, as depicted in Figure 1. The upper surface is held at a temperature T_c while the lower one is at $T_h (> T_c)$. It is assumed that both form-drag and boundary effects are significant, that the porous medium is isotropic but that local thermal equilibrium does not apply. Thus the governing equations, i.e. the continuity equation, a suitably extended Darcy's law and the energy equation, subject to the Boussinesq approximation, take the forms

$$\nabla \cdot \mathbf{V} = 0 \tag{1}$$

$$\frac{\rho_f}{\varepsilon}\frac{\partial \mathbf{V}}{\partial t} + \frac{\rho_f}{\varepsilon^2}\mathbf{V}\cdot\nabla\mathbf{V} = -\nabla p + \mu_e \nabla^2 \mathbf{V} - \frac{\mu_f}{K}\mathbf{V} + \rho_f g \beta (T - T_c)\mathbf{y} - \frac{\rho_f b}{\sqrt{K}}\mathbf{V}|\mathbf{V}| \tag{2}$$

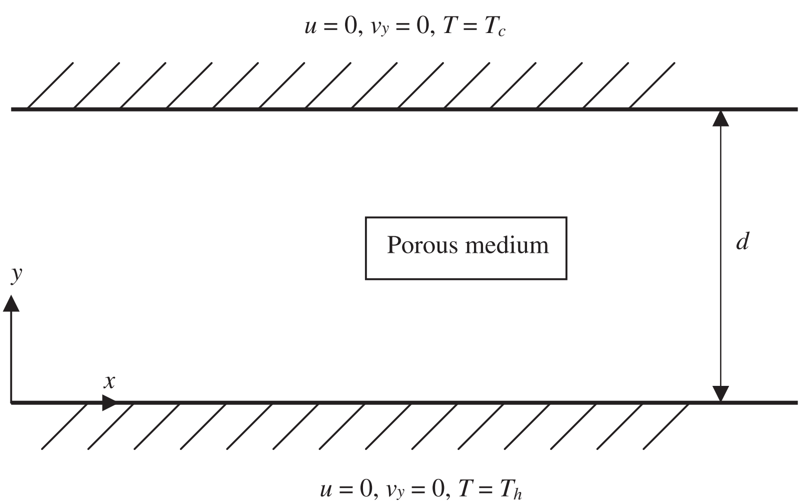

Figure 1. Definition sketch of the horizontal layer.

$$\varepsilon(\rho c)_{\mathrm{f}}\frac{\partial T_{\mathrm{f}}}{\partial t}+(\rho c)_{\mathrm{f}}\mathbf{V}\cdot\nabla T_{\mathrm{f}}=\varepsilon k_{\mathrm{f}}\nabla^{2}T_{\mathrm{f}}+h(T_{\mathrm{s}}-T_{\mathrm{f}}) \tag{3}$$

$$(1-\varepsilon)(\rho c)_{\mathrm{s}}\frac{\partial T_{\mathrm{s}}}{\partial t}=(1-\varepsilon)k_{\mathrm{s}}\nabla^{2}T_{\mathrm{s}}-h(T_{\mathrm{s}}-T_{\mathrm{f}}) \tag{4}$$

The constants and variables used in these equations are defined in the Nomenclature. The boundary conditions are

$$u=0,\ \ v_y=0,\ \ T=T_{\mathrm{h}}\quad \text{at } y=0 \tag{5a}$$

$$u=0,\ \ v_y=0,\ \ T=T_{\mathrm{c}}\quad \text{at } y=d \tag{5b}$$

where the velocity conditions correspond to the stress-free case. Equation (1)–(4) are nondimensionalised using the transformations

$$\tilde{\mathbf{x}}=\frac{1}{d}\mathbf{x},\quad \tilde{\mathrm{t}}=\frac{(\rho c)_{\mathrm{f}}\,d^{2}}{k_{\mathrm{f}}}t,\quad \tilde{\mathbf{V}}=\frac{\varepsilon k_{\mathrm{f}}}{(\rho c)_{\mathrm{f}}\,d}\mathbf{V},$$

$$\tilde{\mathrm{p}}=\frac{\mu k_{\mathrm{f}}}{(\rho c)_{\mathrm{f}}K}\,p,\quad \theta=\frac{T_{\mathrm{f}}-T_{\mathrm{c}}}{T_{\mathrm{h}}-T_{\mathrm{c}}},\quad \varphi=\frac{T_{\mathrm{s}}-T_{\mathrm{c}}}{T_{\mathrm{h}}-T_{\mathrm{c}}} \tag{6}$$

and the governing equations become

$$\nabla\mathbf{V}=0 \tag{7}$$

$$\varepsilon F_1\frac{\partial\mathbf{V}}{\partial t}+F_1\mathbf{V}\cdot\nabla\mathbf{V}=-\varepsilon^{2}F_1\nabla p+D\nabla^{2}\mathbf{V}-\mathbf{V}+R\theta\mathbf{y}-F_2\mathbf{V}|\mathbf{V}| \tag{8}$$

$$\frac{\partial\theta}{\partial t}+\mathbf{V}\cdot\nabla\theta=\nabla^{2}\theta+H(\varphi-\theta) \tag{9}$$

$$\alpha\frac{\partial\varphi}{\partial t}+\mathbf{V}\cdot\nabla\varphi=\nabla^{2}\varphi+\gamma H(\theta-\varphi) \tag{10}$$

where the tildes have been omitted, for convenience of presentation. In Equations (8)–(10), the following constants were introduced:

$$F_1=\frac{\rho_{\mathrm{f}}\kappa K}{\varepsilon^{2}d^{2}\mu_{\mathrm{f}}},\quad F_2=\frac{\rho_{\mathrm{f}}\kappa K^{1/2}}{d\mu_{\mathrm{f}}},\quad D=\frac{\mu_{\mathrm{e}}}{\mu_{\mathrm{f}}}\cdot\frac{K}{d^{2}},$$

$$H=\frac{hd^{2}}{\varepsilon k_{\mathrm{f}}},\quad \gamma=\frac{\varepsilon k_{\mathrm{f}}}{(1-\varepsilon)k_{\mathrm{s}}},\quad \alpha=\frac{(\rho c)_{\mathrm{s}}}{(\rho c)_{\mathrm{f}}}\cdot\frac{k_{\mathrm{f}}}{k_{\mathrm{s}}} \tag{11}$$

and $R=\frac{\rho_{\mathrm{f}}g\beta(T_{\mathrm{h}}-T_{\mathrm{c}})Kd}{\varepsilon\mu_{\mathrm{f}}k_{\mathrm{f}}}$ is the Darcy–Rayleigh number based on the fluid properties. We note that the usual Rayleigh number, which is based on the mean properties of the porous medium is given by $\mathrm{R}\gamma/(1+\gamma)$. The boundary conditions (5) become

$$u=0,\ \ v_y=0,\ \ \theta=\varphi=1\quad \text{on } y=0 \tag{12a}$$

$$u=0,\ \ v_y=0,\ \ \theta=\varphi=0\quad \text{on } y=1 \tag{12b}$$

The basic conduction profile, whose stability is the subject of this short paper, is given by

$$\mathbf{V}=0,\quad \theta=\varphi=1-y \tag{13}$$

We focus our attention to the 2D case and we introduce the stream-function ψ , according to

$$u = -\frac{\partial \psi}{\partial y}, \quad v = \frac{\partial \psi}{\partial x} \tag{14}$$

Here, u and v are the components of the velocity in the Cartesian x (horizontal) and y (spanwise) directions. The basic conduction profile given by (13) are perturbed by setting:

$$\psi = \Psi, \quad \theta = 1 - y + \Theta, \quad \varphi = 1 - y + \Phi \tag{15}$$

and after linearization, we obtain

$$\varepsilon F_1 \frac{\partial}{\partial t}\left(\frac{\partial^2 \Psi}{\partial x^2} + \frac{\partial^2 \Psi}{\partial y^2}\right) + \frac{\partial^2 \Psi}{\partial x^2} + \frac{\partial^2 \Psi}{\partial y^2} - D\left(\frac{\partial^4 \Psi}{\partial x^4} + 2\frac{\partial^4 \Psi}{\partial x^2 \partial y^2} + \frac{\partial^4 \Psi}{\partial y^4}\right) = R\frac{\partial \Theta}{\partial x} \tag{16}$$

$$\frac{\partial \Theta}{\partial t} = \frac{\partial^2 \Theta}{\partial x^2} + \frac{\partial^2 \Theta}{\partial y^2} + \frac{\partial \Psi}{\partial x} + H\,(\Phi - \Theta) \tag{17}$$

$$\alpha \frac{\partial \Phi}{\partial t} = \frac{\partial^2 \Phi}{\partial x^2} + \frac{\partial^2 \Phi}{\partial y^2} + \gamma H(\Theta - \Phi) \tag{18}$$

It is easy to show that system (16)–(18) obeys the principle of exchange of stabilities. Consequently, we may set the time derivatives to zero and the problem becomes

$$-D\left(\frac{\partial^4 \Psi}{\partial x^4} + 2\frac{\partial^4 \Psi}{\partial x^2 \partial y^2} + \frac{\partial^4 \Psi}{\partial y^4}\right) + \frac{\partial^2 \Psi}{\partial x^2} + \frac{\partial^2 \Psi}{\partial y^2} = R\frac{\partial \Theta}{\partial x} \tag{19}$$

$$\frac{\partial^2 \Theta}{\partial x^2} + \frac{\partial^2 \Theta}{\partial y^2} + \frac{\partial \Psi}{\partial x} + H\,(\Phi - \Theta) = 0 \tag{20}$$

$$\frac{\partial^2 \Phi}{\partial x^2} + \frac{\partial^2 \Phi}{\partial y^2} + \gamma H\,(\Theta - \Phi) = 0 \tag{21}$$

subject to

$$\Psi = \Theta = \Phi = 0, \quad \frac{\partial^2 \Psi}{\partial y^2} = 0, \quad \text{on } y = 0 \text{ and } y = 1 \tag{22}$$

Equations (19)–(22) admit solutions in the form

$$\Psi = A_1 \cos kx \sin \pi y, \quad \Theta = A_2 \sin kx \sin \pi y, \quad \Phi = A_3 \sin kx \sin \pi y \tag{23}$$

where k is the horizontal wave number and the A-coefficients are constants. By substituting (23) into Equations (19)–(21), the following set of equations is obtained:

$$\left[(k^2 + \pi^2) + D(k^2 + \pi^2)^2\right] A_1 + kRA_2 = 0 \tag{24}$$

$$kA_1 + (k^2 + \pi^2 + H)A_2 - HA_3 = 0 \tag{25}$$

$$-\gamma HA_2 + (k^2 + \pi^2 + \gamma H)A_3 = 0 \tag{26}$$

The condition that this homogeneous system has non-trivial solutions leads to an eigenvalue equation for R in terms of k, D, H and γ. After some algebra, we obtain

$$R = (\pi^2 + k^2)^2[1 + D(\pi^2 + k^2)] \cdot \frac{\pi^2 + k^2 + H(\gamma + 1)}{k^2(\pi^2 + k^2 + \gamma H)} \tag{27}$$

In the remainder of the paper we determine not only the variation of R with k for selected values of H , D and γ but we minimize R with respect to k in order to find the smallest Rayleigh number at which convection may be expected. In Section 3 we consider the extreme cases of small H (i.e. for very poor inter-phase heat transport) and large H (i.e. for the local thermal equilibrium limit). In Section 4 we present exact numerical values for R and the minimizing value of k.

3. ASYMPTOTIC ANALYSIS FOR BOTH SMALL AND LARGE VALUES OF *H*

3.1. Small H analysis

We first perform a small-H series expansion of the expression given by (27) to obtain

$$R = \frac{1 + D(\pi^2 + k^2)}{k^2}\left[(\pi^2 + k^2)^2 + (\pi^2 + k^2)H - \gamma H^2 + \cdots\right] \tag{28}$$

which is correct to $O(H^2)$. The minimum value of R is found by setting $\partial R/\partial k = 0$ in (28) and this leads to

$$(1 + D\pi^2)(k^4 - \pi^4) + (\pi^2 + k^2)\left[2Dk^4 - H(1 + D\pi^2)\right] + (1 + D\pi^2)H(k^2 + \gamma H) + Dk^4 H + \cdots = 0 \tag{29}$$

When $D = 0$, the Darcy flow limit, Equation (29) reduces to $(k^4 - \pi^4) - \pi^2 H + \gamma H^2 + \cdots = 0$ which is in agreement with Eq. (13) from Banu and Rees (2002). By expanding k using the expansion,

$$k = k_0 + k_1 H + k_2 H^2 + \cdots \tag{30}$$

and inserting (30) in (29), we obtain at $O(H^0)$

$$(1 + D\pi^2)(k_0^2 - \pi^2) + 2k_0^4 D = 0 \tag{31}$$

For $D = 0$, this equation gives $k_0 = \pi$ immediately, in agreement with Equation (14) from Banu and Rees (2002). Equation (31) yields the solution

$$k_0 = \pi\left[2(1 + D^2\pi^2)\right]^{1/2}\left[1 + D\pi^2 + (1 + 10\pi^2 D + 9\pi^4 D^2)^{1/2}\right]^{-1/2} \tag{32}$$

which is valid for all values of D.

At $O(H)$ we get

$$k_1 = \frac{\pi^2 + D(\pi^4 - k_0^4)}{4k_0^3(1 + 3D\pi^2 + 3k_0^2 D)} \tag{33}$$

while at $O(H^2)$,

$$k_2 = \left\{ 6k_0^2k_1^2[1 + \pi^2(D+1) + k_0^2] + 2k_0^4k_1^2D + (1 + D\pi^2)(2k_0k_1 + \gamma) + 4Dk_0^3k_1 \right\}$$
$$\times (2k_0^3)^{-1}\left[2(1 + D\pi^2) + 2(\pi^2 + k_0^2) + Dk_0^2\right]^{-1} \tag{34}$$

In conclusion, the critical wave number k_c is given by (30), while the critical Rayleigh number is given by (28).

3.2. Large H analysis

For large values of H, R takes the form

$$R = \frac{(\pi^2 + k^2)^2[1 + D(\pi^2 + k^2)]}{k^2} \cdot \frac{\gamma + 1}{\gamma} \cdot \left[1 - \frac{\pi^2 + k^2}{\gamma(\gamma+1)}\frac{1}{H} + \frac{(\pi^2+k^2)^2}{\gamma^2(\gamma+1)}\frac{1}{H^2} + \cdots\right] \tag{35}$$

On minimizing with respect to k, we obtain

$$\frac{\gamma+1}{\gamma}\left[k^2 - \pi^2 + D(2k^4 + \pi^2k^2 - \pi^4)\right] - \frac{\pi^2 + k^2}{\gamma^2 H}\left[2k^2 - \pi^2 + D(3k^4 + 2\pi^2k^2 - \pi^4)\right]$$
$$+ \frac{(\pi^2+k^2)^2}{\gamma^3H^2}\left[3k^2 - \pi^2 + D(4k^4 + 3\pi^2k^2 - \pi^4)\right] = 0 \tag{36}$$

We notice that, when $D = 0$, Equation (36) reduces to (18) from Banu and Rees (2002). By expanding k in terms of inverse powers of H we also obtain,

$$k = k_0 + \frac{k_1}{H} + \frac{k_2}{H^2} + \cdots \tag{37}$$

After inserting (37) into (36) the $O(1)$ terms yield the expression.

$$k_0^2 - \pi^2 + D(2k_0^4 + \pi^2k_0^2 - \pi^4) = 0$$

For $D = 0$, this equation gives also $k_0 = \pi$. In the general case we again have to apply (32). At $O(1/H)$ we get

$$k_1 = (2k_0)^{-1}\left[1 + D(4k_0^2 + \pi^2)\right]^{-1}(\pi^2 + k_0^2)\cdot\left[3Dk_0^4 + 2(1 + \pi^2D)k_0^2 - \pi^2(1 + \pi^2D)\right] \tag{38}$$

Further, at $O(1/H^2)$, we obtain

$$k_2 = \frac{A}{2k_0(4Dk_0^2 + 1 + D\pi^2)} \tag{39}$$

where

$$A = -k_1^2(12Dk_0^2 + 1 + D\pi^2) + \frac{2k_0k_1}{\gamma(\gamma+1)}\left[2(\pi^2 + k_0^2)\cdot(3Dk_0^2 + 1 + D\pi^2)\right.$$
$$\left. + k_0^2(Dk_0^2 + 1 + D\pi^2)\right] - \frac{2k_0^2}{\gamma^2(\gamma+1)}(\pi^2 + k_0^2)^2(Dk_0^2 + 1 + D\pi^2)$$

In conclusion, the critical wave number k_c is given by (37), whilst the critical Rayleigh number is given by (35).

4. NUMERICAL RESULTS

With the aim to find the critical wavenumber, which corresponds to the minimum Rayleigh number, we calculate $\partial R/\partial k = 0$, and on using (27), we get

$$\left[k^2 - \pi^2 + D(2k^4 - \pi^4 + k^2\pi^2)\right]\left[\pi^2 + k^2(1+\gamma)H\right] \times (\pi^2 + k^2 + \gamma H) - k^2 H(\pi^2 + k^2)\left[1 + D(\pi^2 + k^2)\right] = 0 \quad (40)$$

Eq. (40) reduces, in the case when $D = 0$, to Eq. (21) from Banu and Rees (2002). Eq. (40) gives the critical value of k (for various values of H, γ and D), which, when inserted into (27), provides the critical value of the Rayleigh number.

Figure 2 gives a selection of neutral curves (R against k/π) for various values of γ and D with $H = 100$. These all follow the familiar shape for Benard-like problems with a single well-defined minimum value. There is a general trend towards the values of R becoming smaller as D decreases and as γ increases. The size of D is related to the importance of viscous effects at the

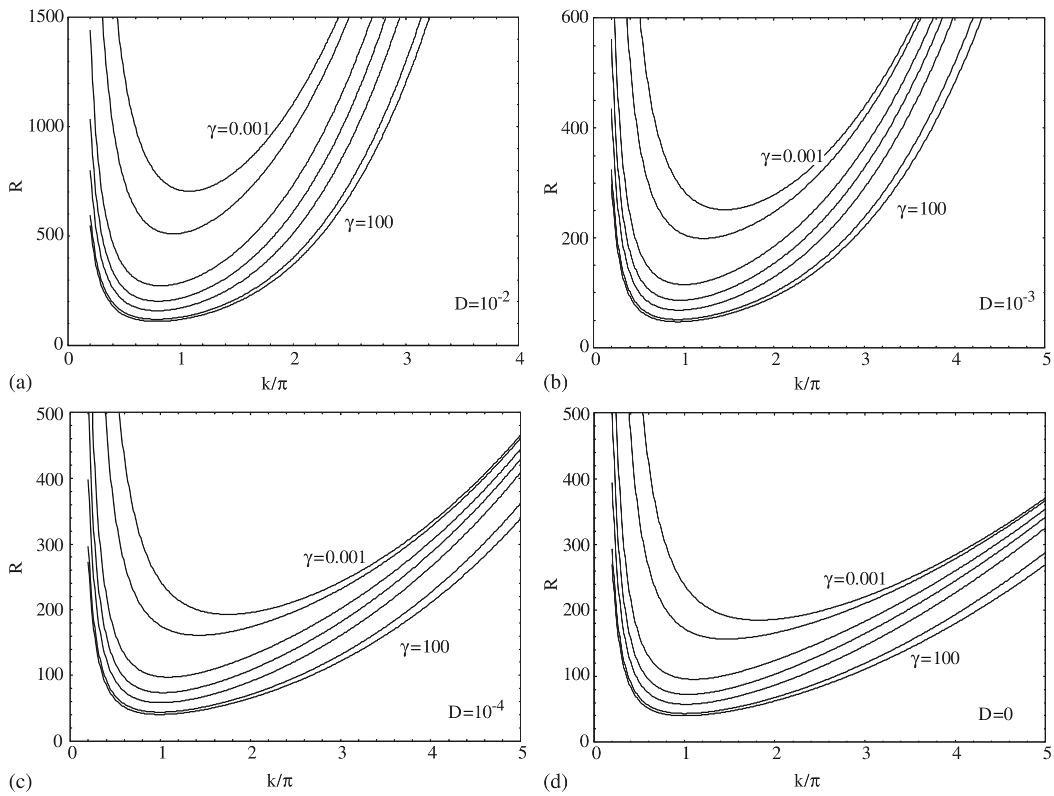

Figure 2. Neutral curves for $H = 100$, $\gamma = 0.001$, 0.01, 1, 5, 10, 50 and 100: (a) $D = 10^{-2}$; (b) $D = 10^{-3}$; (c) $D = 10^{-4}$; (d) $D = 0$.

Table I. Comparison of the exact and asymptotic values of the wave number and the critical Rayleigh number for large H and $\gamma = 1$. "E" denotes the exact solution and "A" the asymptotic solution.

$\log_{10} H$	k_c(E)	k_c(A)	R_c(E)	R_c(A)
$D = 0$				
1.5	3.40956		63.40428	
2	3.27061		72.33957	
2.5	3.18795	3.18416	76.62136	76.63087
3	3.15683	3.15645	78.19083	78.19114
3.5	3.14647	3.14643	78.71175	78.71176
4	3.14314	3.14314	78.87904	78.87904
4.5	3.14208	3.14208	78.93221	78.93221
5	3.14175	3.14175	78.94904	78.94904
$D = 10^{-6}$				
1.5	3.40952		63.40564	
2	3.27057		72.34106	
2.5	3.18792	3.18412	76.62289	76.63240
3	3.15680	3.15641	78.19239	78.19269
3.5	3.14644	3.14639	78.71330	78.71331
4	3.14311	3.14310	78.88060	78.88060
4.5	3.14205	3.14204	78.93376	78.93376
5	3.14172	3.14171	78.95060	78.95060
$D = 10^{-5}$				
1.5	3.40911		63.41791	
2	3.27023		72.35445	
2.5	3.18762	3.18377	76.63671	76.63922
3	3.15651	3.15606	78.20634	78.20665
3.5	3.14616	3.14604	78.72731	78.72732
4	3.14283	3.14275	78.89462	78.89462
4.5	3.14177	3.14169	78.94779	78.94779
5	3.14144	3.14136	78.96463	78.96463
$D = 10^{-4}$				
1.5	3.40512		63.54047	
2	3.26686		72.48826	
2.5	3.18463	3.18019	76.77477	76.78430
3	3.15367	3.15254	78.34585	78.34616
3.5	3.14336	3.14255	78.86728	78.86730
4	3.14005	3.13927	79.03474	79.03474
4.5	3.13899	3.13822	79.08796	79.08796
5	3.13866	3.13788	79.10481	79.10481
$D = 10^{-3}$				
1.5	3.36726		64.75793	
2	3.23474		73.81881	
2.5	3.15609	3.14560	78.14846	78.15857
3	3.12642	3.11852	79.73422	79.73504
3.5	3.11654	3.10880	80.26042	80.26094
4	3.11337	3.10561	80.42940	80.42991
4.5	3.11236	3.10459	80.48310	80.48362
5	3.11204	3.10427	80.50011	80.50062

Table II. Comparison of the exact and asymptotic values of the wave number and the critical Rayleigh number for small H and $\gamma = 1$. "E" denotes the exact solution and "A" the asymptotic solution.

$\log_{10} H$	k_c(E)	k_c(A)	$R_c(E)$	R_c(A)
$D = 0$				
−2	3.14239	3.14239	39.49480	39.49740
−1.5	3.14410	3.14411	39.54154	39.53844
−1	3.14944	3.14951	39.67716	39.66808
−0.5	3.16569	3.16640	40.09856	40.07684
0	3.21132	3.21756	41.36210	41.35770
0.5	3.31346		44.80466	
1	3.43635		52.35964	
$D = 10^{-6}$				
−2	3.14235	3.14235	39.49918	39.49818
−1.5	3.14407	3.14407	39.54232	39.53922
−1	3.14941	3.14948	39.67795	39.66887
−0.5	3.16566	3.16636	40.09936	40.07764
0	3.21128	3.21752	41.36293	41.35854
0.5	3.31342		44.80560	
1	3.43630		52.36077	
$D = 10^{-5}$				
−2	3.14208	3.14200	39.50620	39.50520
−1.5	3.14379	3.14372	39.54935	39.54625
−1	3.14913	3.14913	39.68501	39.67593
−0.5	3.16537	3.16600	40.10654	40.08480
0	3.21099	3.21716	41.37045	41.36605
0.5	3.31309		44.81400	
1	3.43951		52.37099	
$D = 10^{-4}$				
−2	3.13930	3.13852	39.57635	39.57535
−1.5	3.14100	3.14024	39.61961	39.61650
−1	3.14633	3.14563	39.75564	39.74652
−0.5	3.16253	3.16248	40.17828	40.15646
0	3.20801	3.21353	41.44553	41.44108
0.5	3.30977		44.89802	
1	3.43201		52.47307	
$D = 10^{-3}$				
−2	3.11267	3.10489	40.27456	40.27377
−1.5	3.11433	3.10658	40.31896	40.31598
−1	3.11952	3.11188	40.45896	40.44933
−0.5	3.13531	3.12842	40.89229	40.86980
0	3.17956	3.17853	42.19264	42.18783
0.5	3.27814		45.73351	
1	3.39494		53.48720	

boundaries, and reductions in D decrease this effect, which allows the fluid to move more easily, thereby decreasing the critical Rayleigh number. Large values of γ mean that heat is transported through both the solid and fluid phases, whereas small values correspond to transport primarily through the fluid phase. Thus convection is established more readily for larger values of γ when

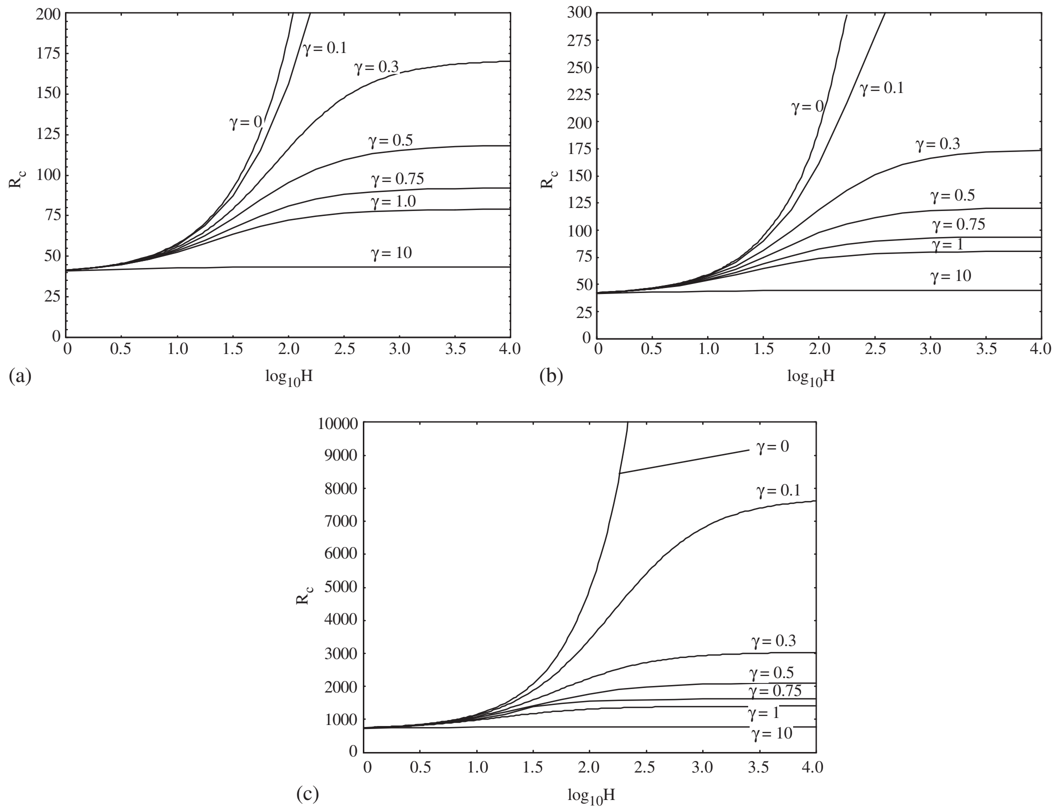

Figure 3. Variation of the critical Rayleigh number R_c with $\log_{10} H$, for various values of γ: (a) $D = 0$; (b) $D = 10^{-3}$; (c) $D = 1$.

all other parameters are held fixed. A similar argument may be put forward for the variation in R when H varies, since H measures the ease with which heat is transferred between the phases.

The LTE case is recovered in the large H-limit. In Table I are provided comparisons, in the LTE limit, of the exact and asymptotic values of the critical wavenumber and the critical Rayleigh number for large H with $\gamma = 1$. Agreement between the asymptotic results and the exact solutions are very good, especially for the larger values of H. However, as the value of D increases, agreement reduces slightly for any fixed value of H.

In Table II are presented the exact and asymptotic values of the wavenumber and the critical Rayleigh number for small values of H (the non LTE case) with $\gamma = 1$. We have increasingly good agreement as H decreases, but, for fixed values of H the agreement becomes poorer as D increases.

In Figures 3 and 4, respectively, we summarize the behaviour of the critical Rayleigh number and wavenumber, respectively, as functions of H and γ for $D = 0$, $D = 10^{-3}$ and $D = 1$. The variation of R_c with $\log_{10} H$ is depicted in Figure 3. We again see the fact that R_c increases as H increases and γ decreases. When H is small all the curves asymptote to a single value which is independent of γ and given by (32). At the opposite extreme we see, from (35), that the asymptotic values of R are such that $R\gamma/(1 + \gamma)$ attains a value which is independent of γ. That

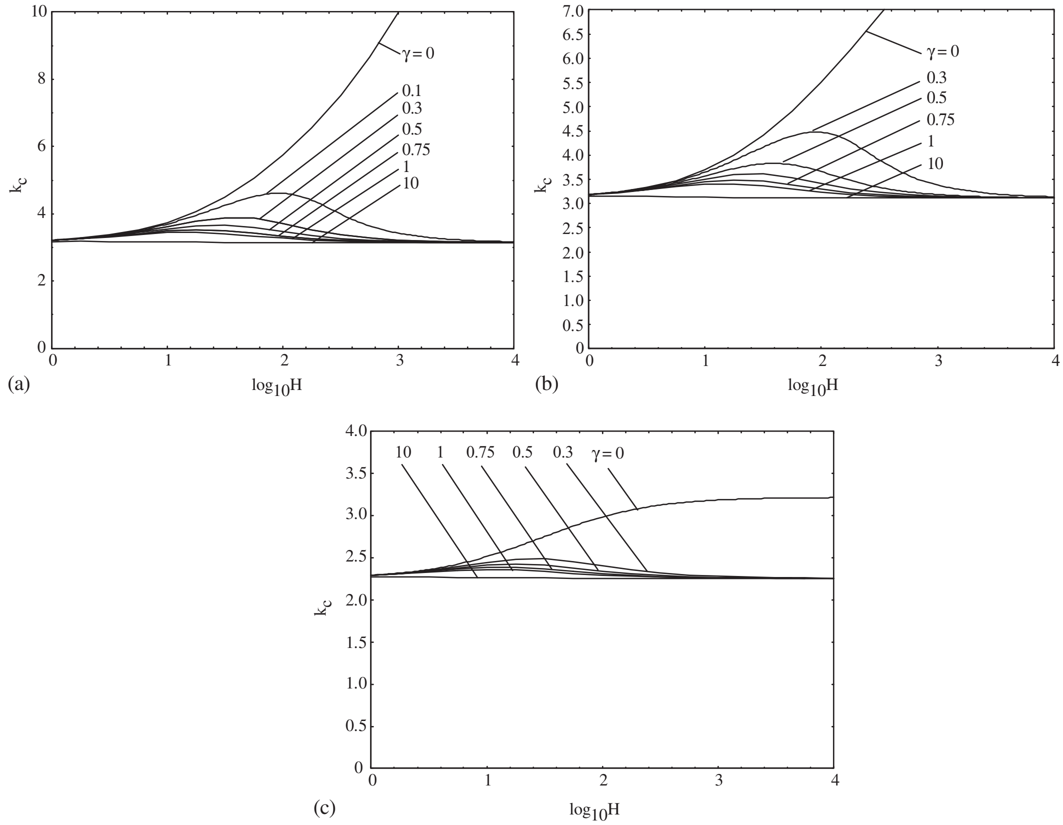

Figure 4. Variation of the critical wave number k_c with $\log_{10}H$, for various values of γ: (a) $D=0$; (b) $D=10^{-3}$; (c) $D=1$.

this should be so is not surprising since the constant, $R\gamma/(1+\gamma)$ precisely the Rayleigh number which is based on the mean properties of the porous medium, rather than on the fluid properties as given in (11).

In Figure 4 we see that k_c attains the value π in both the large and small H limits. At intermediate values of H the value of k_c is larger, and increasingly so as γ increases or as D decreases. That k_c should attain the value π when H is small may be understood from the fact that Equations (19) and (20) form the standard Darcy–Brinkman stability equations (subject to a rescaling of the Rayleigh number) and that the equation for the solid phase temperature decouples from (19) and (20). Therefore we would expect the wave number to take that value when there is no microscopic conduction between the phases.

5. CONCLUSIONS

In this paper we have analysed in detail the combined effects of boundary (Brinkman) and non LTE on the onset of convection in a porous layer of infinite extent. Although we have also included inertia effects in the formulation, their presence does not affect the stability criterion, since the basic state is motionless. With the aim of undertaking an analytical study, we have considered the case of stress free boundaries. This restriction has been relaxed in Rees and Postelnicu (2002).

The present study shows that variations in the values of H, γ and D have a significant effect on the criterion for the onset of convection. Detailed numerical and asymptotic solutions have been presented for R_c and k_c as functions of D, H and γ. As in Banu and Rees (2002), it has been shown that LTE is recovered in the large H limit.

On the other hand, at fixed values of γ and H, the critical wave number k_c reduces and the critical Rayleigh number R_c increases as D increases. Conversely, at fixed D, the convection onset occurs at lower values of R as H decreases or γ increases.

NOMENCLATURE

b	= form drag coefficient
c	= specific heat
d	= depth of the convection layer
D	= Darcy number
F_1, F_2	= dimensionless coefficients
g	= gravity
h	= inter-phase heat transfer coefficient
H	= scaled inter-phase heat transfer coefficient
k	= wave number
K	= permeability
LTE	= Local thermal equilibrium
P	= Pressure
R	= Darcy–Rayleigh number
t	= Time
u, v	= fluid flux velocities
$\mathbf{V}$	= dimensional velocity vector
x, y	= Cartesian co-ordinates

Greek letters

α	= diffusivity ratio
β	= coefficient of expansion
ρ	= density
κ	= diffusivity
ε	= porosity
μ	= viscosity
ψ	= streamfunction
θ,Θ	= scaled temperature of the fluid phase
φ,Φ	= scaled temperature of the solid phase
γ	= porosity-scaled conductivity ratio

Superscipts and subscripts

c = cold or critical
e = effective (viscosity)
f = fluid
h = hot
s = solid
$'$ = η-derivative
0,1,2 = successive terms in series expansions

REFERENCES

Horton CW, Rogers FT. 1945. Convection currents in a porous medium. *Journal of Applied Physics* **16**:367–370.

Lapwood ER. 1948. Convection of a fluid in a porous medium. *Proceeding of the Cambridge Philosophical Society* **44**:508–521.

Schumann TEW. 1929. Heat transfer: a liquid flowing through a porous prism. *Journal of Franklin Institute* **208**:405–416.

Vafai K, Amiri A. 1998. Non-Darcian effects in confined forced convective flows. In Ingham DB, Pop I (eds), *Transport Phenomena in Porous Media*, 313–329.

Kuznetsov AV. 1998. Thermal non-equilibrium forced convection in porous media. In Ingham DB, Pop I (eds.), *Transport Phenomena in Porous Media*, 103–129.

Combarnous M. 1972 Description du transfert de chaleur par convection naturelle dans une couche poreuse horizontale a l'aide d'un coefficient de transfert solide-fluide. *Comptes Rendues des Seances de l'Academie des Sciences, Serie II Paris* **A275**:1375–1378.

Banu N, Rees DAS. 2002. Onset of Darcy–Benard convection using a thermal nonequlibrium model. *International Journal of Heat and Mass Transfer* **45**:2221–2228.

Rees DAS, Postelnicu A. 2002. The onset of a Darcy–Brinkman convection using a thermal nonequlibrium model. Part II, in preparation.

